A SINGLE MASK SOI MECHANICAL VOLTAGE PUMP

Brian Otis, Richard Lu
UC Berkeley

Abstract- A mechanical voltage pump was designed in a single mask SOI process. Theoretical and practical analyses of the operation of the mechanical voltage pump are presented. A design is proposed and possible applications of this design are discussed. Lastly, a comprehensive test structure array was designed.

I. INTRODUCTION

Much of today's MEMs actuation is electrostatically driven. This method is often preferred over thermal actuation for a variety of reasons, including power efficiency, bandwidth, ease of implementation, and the ability to maintain actuator state without power dissipation. However, to achieve high electrostatic forces, it is usually necessary to apply relatively high voltage potentials to conductive beams. CMOS charge pumps have been well documented [1]. However, it is difficult to generate extremely high voltages using modern CMOS processes where the gate and junction breakdown voltages can be as low as 2V and 15V, respectively [2][3]. Therefore, it is advantageous to generate high voltages using a mechanical charge pump residing on the same substrate as the MEMs structures. This allows a maximum voltage equal to the minimum air breakdown voltage (approximately 200V as predicted by the Paschen Curve). The goal of this research is to design and implement a mechanical voltage pump using a simple single mask SOI process that operates from a 5V power source.

II. ANALYSIS

A. Voltage Pump

The voltage multiplication is performed by placing a charge on a variable MEMs capacitor and subsequently decreasing the capacitance while holding the charge constant. A conceptual diagram is shown below.

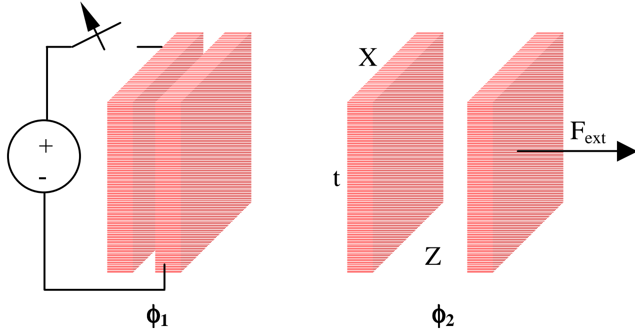

Figure 1. Conceptual diagram of voltage pump

In ϕ_1, the plates are in close proximity, and a voltage potential V_1 is applied to them and then removed, placing a charge $Q_{initial}$ on the plates. In ϕ_2, the plates are separated from each other with external force F_{ext}. Thus, the capacitance between the plates decreases. A few simple equations demonstrate the voltage multiplication:

$$Q_{initial} = C_{initial} V_{initial} \qquad (1)$$
$$Q_{final} = C_{final} V_{final}$$

Charge is conserved as the plates are separated.

$$Q_{initial} = Q_{final} \rightarrow V_{final} = V_{initial} \left(\frac{C_{initial}}{C_{final}}\right) \qquad (2)$$

Therefore,

$$V_{final} = V_{initial} \left(\frac{Z_{final}}{Z_{initial}}\right) \qquad (3)$$
$$M = \frac{C_{initial}}{C_{final}} = \frac{V_{final}}{V_{initial}}$$

Where M is the voltage multiplication factor and C_{final} is the capacitor that holds the multiplied voltage. Since the charge $V_{final}*C_{final}$ is ultimately shared with the electrostatic MEMs structures, it is important to choose C_{final} large enough to minimize the effects of charge sharing. Additionally, any actual implementation will have parasitic capacitances that will degrade M. In this design, parasitics are defined as any capacitance that remains constant as the plates are separated. As shown in the equations below, the parasitic capacitance C_p degrades the voltage multiplication factor.

$$V_{final} = V_{initial} \left(\frac{C_{initial} + C_p}{C_{final} + C_p}\right) \qquad (4)$$

It can be easily verified that:

$$M' = \frac{V_{final}}{V_{initial}} = M \left(\frac{C_{final}}{C_{final} + C_p}\right), \quad if\ C_{final} >> C_p \qquad (5)$$

Where M' is our modified voltage multiplication factor.

B. MEMs Structure

The physical structure includes the voltage pump plates, the actuator to move the plates, and the mechanical suspension to allow plate movement. There are multiple methods of obtaining a variable capacitor. One is to slide one plate away from the other laterally with a comb drive [4]. Another method was employed that made use of mechanical resonance to achieve a greater initial displacement [5] using comb drive resonators described in [6]. Yet another method is to use a gap closing actuator to displace the shuttle initially, with the variable capacitor implemented as fingered plates (see Figure 2 below). During ϕ_1, the inner voltage pump plate is deflected by a gap closing actuator towards one of the comb fingers. A voltage source is momentarily applied, causing a charge Q

to be placed on the voltage pump plates. Then, in ϕ_2, a mechanical spring returns the voltage pump plate to its initial position, thereby causing a decrease in total capacitance, and thus, a voltage gain.

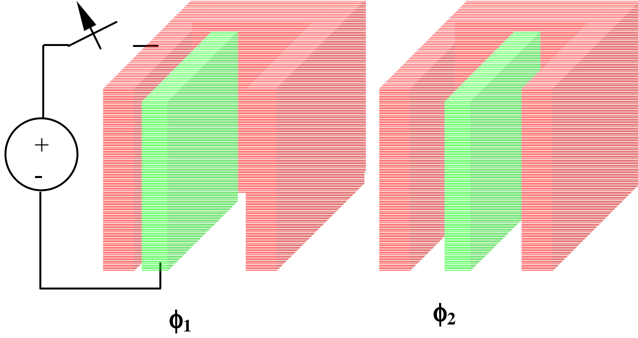

ϕ_1 ϕ_2

Figure 2. Diagram of voltage pump plates

The capacitance of this structure is:

$$C(z) = \frac{\varepsilon_0 Area}{G} \quad (6)$$

Where the effective gap G can be shown to be:

$$G(z) = \frac{1}{2} g\left(1 - \frac{z^2}{g^2}\right) \quad (7)$$

Where g is the initial gap between the fingers and z is the displacement of the inner plates. The method shown above is desirable because the force required to pull the inner plate back is *linear* with its displacement. For N fingers, the following equations can be derived:

$$\begin{aligned} F_T(z) &= F_1(z) + F_2(z) \\ F_1(z) &= \frac{-1}{2}\varepsilon_0 V(z)^2 \frac{tL}{(g-z)^2} \\ F_2(z) &= \frac{1}{2}\varepsilon_0 V(z)^2 \frac{tL}{(g+z)^2} \\ V(z) &= V_i \frac{C_i}{C(z)} \end{aligned} \quad (8)$$

$$\therefore, F_T(z) = \frac{C_i^2 V_i^2 z}{2NtL\varepsilon_0 g} \quad (9)$$

This system has an equivalent spring constant:

$$K_{eq} = \frac{C_i^2 V_i^2}{2NtL\varepsilon_0 g} \quad (10)$$

It is therefore possible to pull the plates apart with a mechanical spring with a spring constant:

$$|K_{spring}| > |K_{eq}| \quad (11)$$

This system provides a voltage gain of

$$\frac{V_{final}}{V_i} = \frac{C_i}{C_f} = \frac{1}{2}\left[\frac{g}{g - z_{def}} + \frac{g}{g + z_{def}}\right] = \left(1 - \frac{z_{def}^{\ 2}}{g^2}\right)^{-1} \quad (12)$$

where z_{def} is the pre-loaded deflection of the plates and g is the initial finger gap. As described in the previous section, this voltage gain is degraded by any parasitic capacitance in the system.

III. IMPLEMENTATION

A. Process

To achieve a high capacitance per unit area, an SOI process is desirable. In addition, to create a reliable and robust design, a single mask process was used. Some relevant process parameters are shown below in Table 1:

Table 1. Relevant Process Parameters

Process Parameter	*Value*
Structual silicon thickness	50µm
Sheet resistance	1k Ω/
SiO_2 thickness	2µm
Minimum gap	2µm
Minimum feature width	4µm
E_{scs} [7]	~170Gpa

B. Voltage pump design

To realize this mechanism in the process shown in Table 1, the following design was chosen (see Figure 3. below).

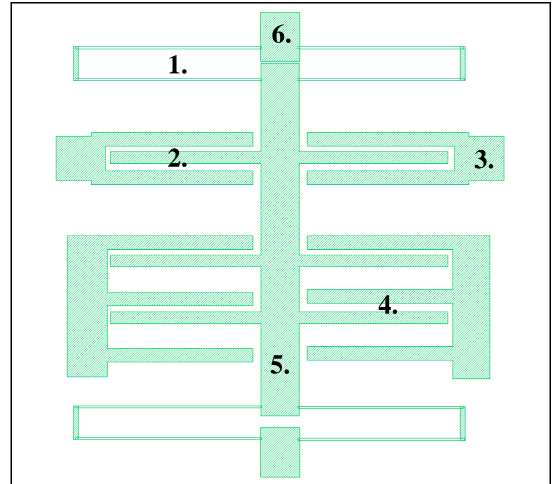

Figure 3. Simplified Mechanical Structure

The simplified structure above consists of five main components:

1. Suspension consisting of four folded-beam springs.
2. Voltage pump capacitors (only one finger shown)
3. Voltage pump anchors.
4. Gap closing actuators (two fingers shown) are used to pre-load the mechanical spring.
5. Main shuttle (electrically grounded through the suspensions).
6. Shuttle gap-stop

As shown in equations (4) & (5), the voltage gain is degraded by the parasitic capacitance. This degradation is mitigated by increasing the value of C_{final}. However, as shown in equation (9), increasing C_{final} (and, therefore, $C_{initial}$) increases the effective spring constant of the voltage pump mechanism, thereby increasing the mechanical spring constant necessary to overcome this force for a given voltage gain. Increasing the mechanical spring constant, in turn, requires a larger actuation structure to initialize the system. This is a fundamental tradeoff of the system. With this in mind, the following design methodology was used.

The first step is to estimate $C_{parasitic}$. This is a process dependent value that allows the designer to choose $C_{initial}$ for a desired voltage gain. The main sources of parasitic capacitance of the structure in Figure 3 are the voltage pump anchors. Thus, the following is a general expression for the lower bound of $C_{parasitic}$ for this design:

$$W_{effectuve} = W_{drawn} - 2W_{overetch}$$
$$C_{parasitic} = 2\left[\varepsilon_0\varepsilon_{ox}\frac{(W_{effective})^2}{t_{ox}} + \varepsilon_0\varepsilon_{air}\frac{(W_{drawn})^2 - (W_{effective})^2}{t_{ox}}\right] \quad (13)$$

For this SOI process, the minimum drawn anchor dimensions (W_{drawn}) are 80µm x 80µm. A minimum of two anchors are needed (one for each side of the shuttle). Therefore, assuming a 10µm overetch of the anchors and an oxide thickness of 2µm, the lower bound for $C_{parasitic}$ is 150 fF. The parasitics of the voltage pump fingers also increase $C_{parasitic}$, but for the initial iteration it is neglected due to their relatively small contribution.

According to equation (4), to sustain a voltage gain degradation of no more than 25%, C_{final} must be greater than 450fF. We conservatively designed C_{final} to be 500fF. The length and width of each finger was designed to achieve a high capacitance in a small area while avoiding finger-to-finger pull in. The following equation is crucial in determining the pull-in stability of the fingers:

$$V_{pull-in} = \sqrt{\frac{8k_{finger}g^3}{27\varepsilon_0 A}} = \sqrt{\frac{8Ea^3g^3}{108\varepsilon_0 L^4}} \quad (14)$$

The chosen dimensions were L=310µm and a=5µm (notice that the pull-in voltage is *independent* of the thickness t). Assuming a gap of 1.5µm after pre-loading the spring (to be discussed below), the pull-in voltage is 8V, safely larger than the intended initial voltage of the system. With these dimensions, ten voltage pump fingers were necessary to achieve C_{final}=500fF, assuming an initial finger spacing of 5µm.

To achieve an uncorrected voltage gain of 2, $C_{initial}$ must be >1pF. Given the dimensions specified above, the gap of the pre-loaded structure must be 1.5µm. Since the initial spacing is 5µm, and the pre-loaded gap is 1.5µm, the displacement of the shuttle is 3.5µm.

C. Suspension design

Equation (10) states that the voltage pump, after receiving a constant charge from the source, presents a force opposing the suspension that is equivalent to a spring with constant K_{eq}. Using the values calculated in part B, K_{eq}=1.48. Therefore, to return the shuttle to its initial position after the charge has been applied, the following must hold:

$$\left|K_{suspension}\right| \overset{!}{>} \left|K_{eq}\right| \quad (15)$$

However, the actuator that pre-loads the shuttle must overcome the force presented by the suspension, so careful design is crucial. We chose the target value $K_{suspension}$= -4. The folded beam suspension shown in Figure 3 gives a total mechanical spring constant of:

$$K_{total} = 2\left[\frac{E_{SCS}a^3t}{L^3}\right] \quad (16)$$

where a, t, L are the dimensions of each suspension beam. To reduce the spring area, dimension a was chosen as the lithographic minimum of 4µm. L was chosen to be 600µm in order to meet the target spring constant. It is predicted that process variations on the suspension could cause K_{total} to vary from –3.4 N/m to –5 N/m, with a nominal value of –4N/m.

D. Actuator Design

The chosen actuator topology was a gap-closing actuator with an optimum finger spacing of $\alpha \cong 2.7$. This topology was chosen to produce a predictable actuator and reduce the necessary area. The parasitic capacitance of this structure is not as crucial as on the voltage pump fingers. Finger dimensions of L=310µm and a=5µm were used for area efficiency. To choose the number of fingers, the pull-in voltage of the structure must be less than the intended actuator voltage of 5V. To achieve a conservative pull-in voltage of 3.5V, 32 actuator fingers are used.

E. Final Design

A summary of the design parameters is shown in Table 2 below, and the completed design is shown in Figure 4.

Table 2. Relevant Design Parameters

Design Parameter	*Value*
Voltage pump fingers	10
Actuator fingers	32
$C_{initial}$	1pF
C_{final}	531fF
Displacement	3.5µm
Voltage pump K_{eq}	1.48 N/m
Suspension K	- 4 N/m
$V_{initial}$	5V
V_{final}	8.75V
$f_{resonant}$	3.6 kHz

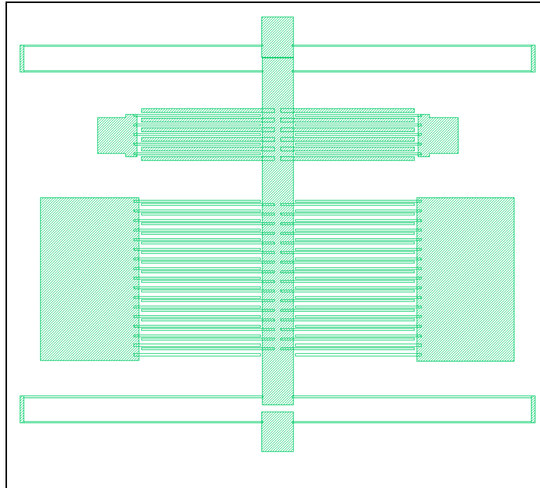

Figure 4. Completed Design

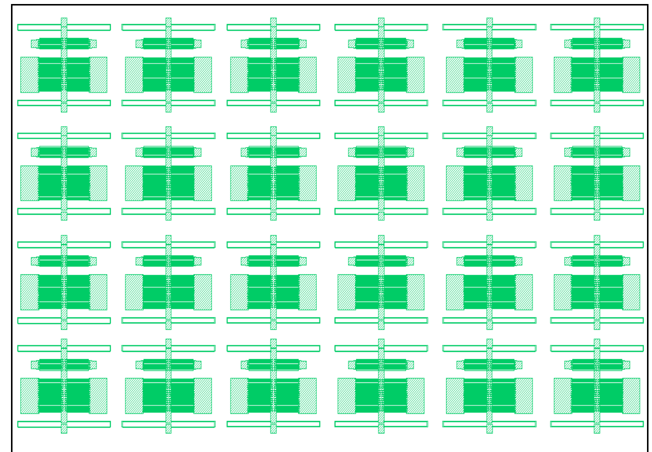

Figure 5. Test Structure Array

V. TEST STRUCTURES

There are two process-dependent parameters that are crucial to the function of the design: the suspension beams and the gap-stop spacing.

If the suspension is too stiff, the gap-closing actuator will need an excessively high voltage to close. If the suspension is too soft, it will not pull the shuttle back into position (equation 15). Moreover, the more accurately this spring constant is known, the more aggressive the design can be. Assumptions made in estimating the Young's Modulus and etching of the structural layer must be validated. In particular, the width (a) of the suspension beams (drawn as 4µm) has a large impact on the mechanical spring constant (proportional to a^3).

Also, an accurate spacing between the shuttle and the gap-stop is imperative. If the gap is too small, the shuttle displacement (and hence, voltage gain) will be small. If the gap is too large, the actuator fingers could collide.

To address these issues, a test structure array, varying from very conservative to very aggressive, was designed. The following table indicates the parameters of the test structures.

Table 3. Test Structure Parameters [a(µm) / g(µm)]

3.5/2	3.8/2	4.1/2	4.4/2	4.7/2	5/2
3.5/2.5	3.8/2.5	4.1/2.5	4.4/2.5	4.7/2.5	5/2.5
3.5/3	3.8/3	4.1/3	4.4/3	4.7/3	5/3
3.5/3.4	3.8/3.4	4.1/3.4	4.4/3.4	4.7/3.4	5/3.4

As shown in the table above, the suspension beam width (a) varies while the gap-stop spacing (g) is held constant (and vise versa). This array provides accurate predictions of the mechanical spring constant and gap-stop spacing for the next iteration of the design. The test structure array layout is shown in Figure 5 below.

VI. CONCLUSION

A single mask SOI mechanical voltage pump has been designed. The intended applications are micro-electromechanical systems where high voltage electrostatic actuation is needed. A test structure array has been designed to characterize sensitive parameters and process variations. Future work includes cascading multiple pumps to achieve higher voltage multiplication ratios, and to utilize mechanical resonance to achieve greater initial displacement.

ACKNOWLEDGMENT

The authors would like to thank Shad Roundy for his valuable advice and suggestions.

REFERENCES

[1] J. Dickson, "On-Chip High-Voltage Generation in MNOS Integrated Circuits using an Improved Voltage Multiplier Techniques," IEEE J. Solid State Circuits, Vol. SC-11, p.374-378, June 1976.

[2] K. Sawada *et al*, "An On-Chip High-Voltage Generator Circuit for EEPROMs with a Power Supply Voltage below 2V," 1995 Symposium on VLSI Circuits, p.75-76

[3] B. Atwood *et al*, "Preliminary Circuits for Smart Dust," 2000 Southwest Symposium on Mixed-Signal Design , San Diego, CA, USA, 27-29 Feb. 2000. IEEE p.87-92

[4] S. Meninger *et al*, "Vibration-to-Electric Energy Conversion," IEEE Transactions on VLSI Systems, Vol. 9, No 1, Feb 2001. p. 64-76.

[5] J. Noworolski and S. Sanders, "Microresonant Devices for Power Conversion," Proceedings of the SPIE - The International Society for Optical Engineering, Vol.3514, SPIE-Int. Soc. Opt. Eng, 1998. p.260-5.

[6] W.C. Tang *et al*, "Laterally Driven Polysilicon Resonant Microstructures," Proceedings of IEEE Micro Electro Mechanical Systems, (IEEE Cat. No.89THO249-3), Salt Lake City, UT, USA, 20-22 Feb. 1989

[7] M. Madou, Fundamentals of Microfabrication, CRC Press, 1997